

Supplementary Material

Facile fabrication of BiOBr-Cu²⁺/TiO₂ suspension for efficient equipment decontamination

Jie Zhang^a, Xuemeng Tian^{b,*}, Chaochao Dong^b, Ruixia Gao^b, Yuan Hu^{a,**}

^aState Key Lab of Fire Science, University of Science and Technology of China, Hefei, 230027, China

^bSchool of Chemistry, Xi'an Jiaotong University, Xi'an, 710049, P.R. China

*Corresponding author.

**Corresponding author.

E-mail address: yuanhu@ustc.edu.cn (Y. Hu), t xm1996@stu.xjtu.edu.cn (X. Tian).

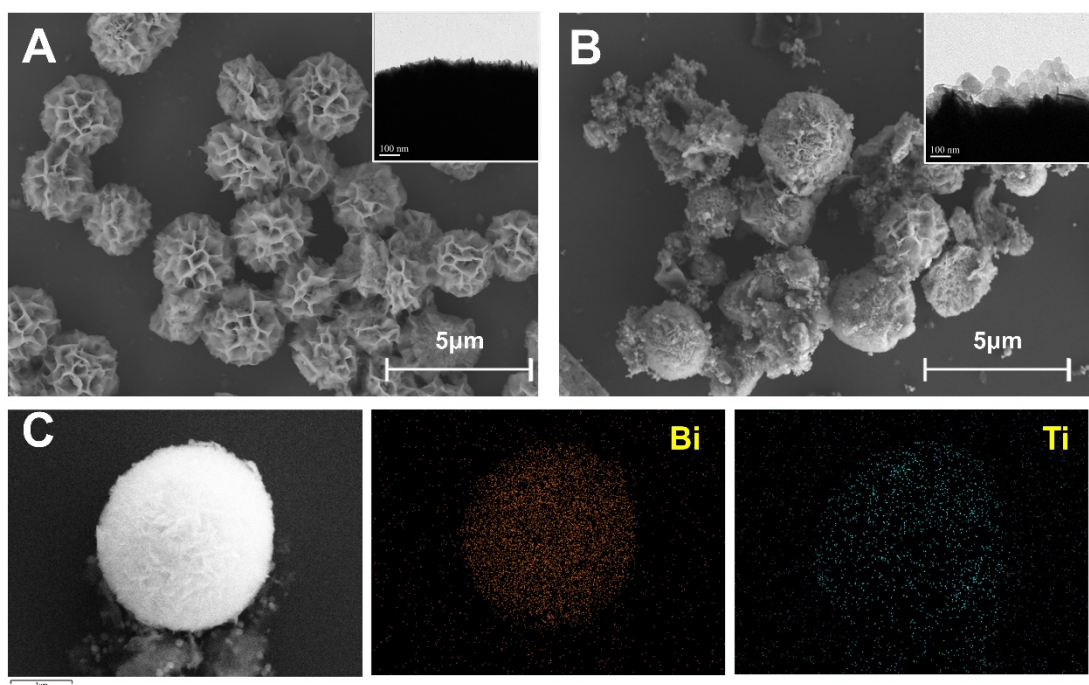


Figure S1 SEM of BiOBr-Cu²⁺ (A) and BiOBr-Cu²⁺/TiO₂ (B) with the inset of corresponding TEM. Elemental mapping of BiOBr-Cu²⁺/TiO₂ (C).

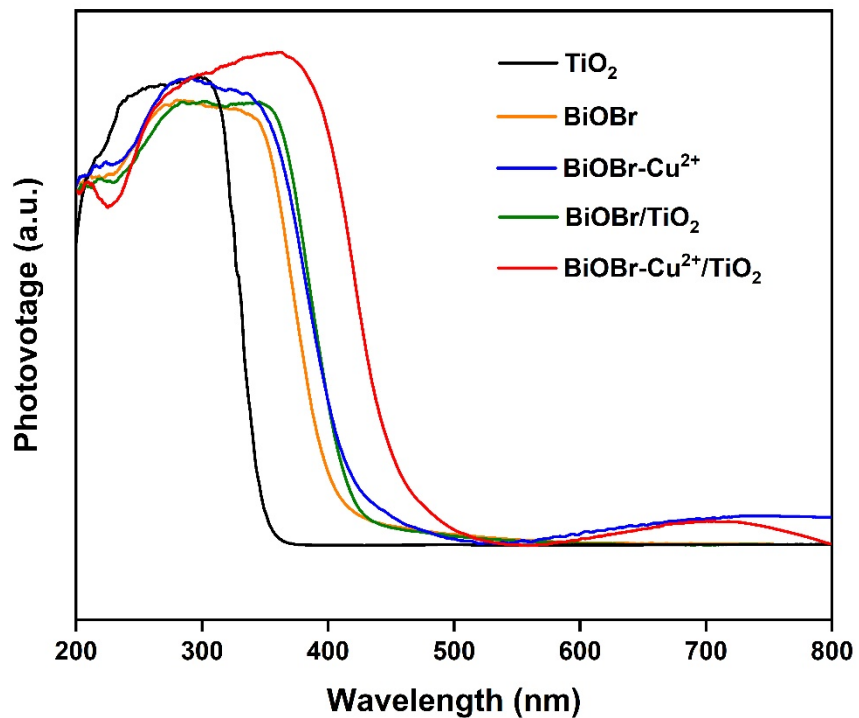


Figure S2 UV-vis DRS of TiO_2 , BiOBr , $\text{BiOBr}-\text{Cu}^{2+}$, $\text{BiOBr}/\text{TiO}_2$, and $\text{BiOBr}-\text{Cu}^{2+}/\text{TiO}_2$.

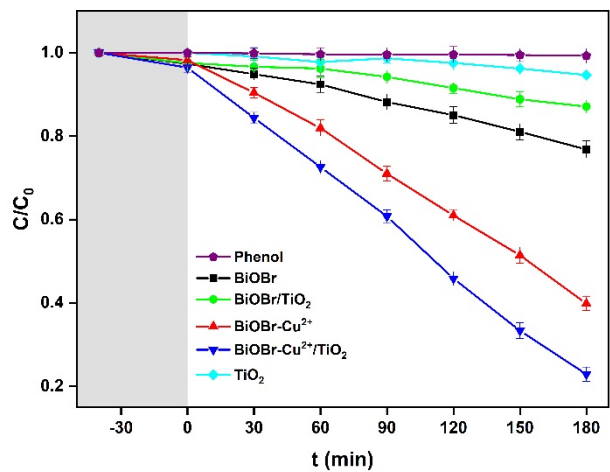


Figure S3 The photodegradation efficiency of phenol on different photocatalysts.

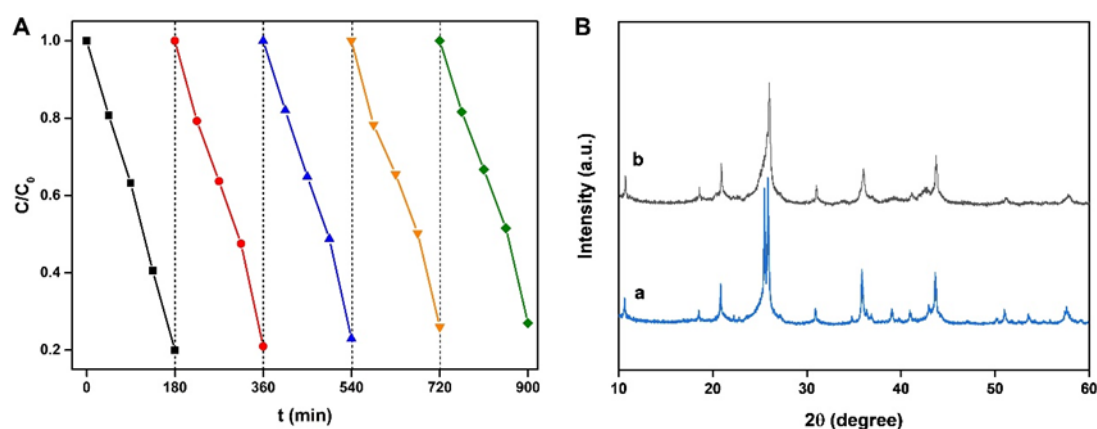


Figure S4. Reusability (A) of $\text{BiOBr-Cu}^{2+}/\text{TiO}_2$ on photodegradation of phenol. XRD pattern (B) for fresh (a) and five-times recycled (b) $\text{BiOBr-Cu}^{2+}/\text{TiO}_2$ sample.

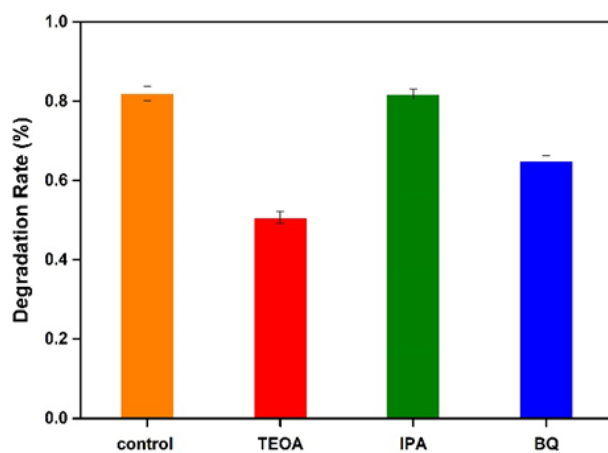


Figure S5. The photocatalytic rate of BiOBr-Cu²⁺/TiO₂ in the presence of different scavengers.

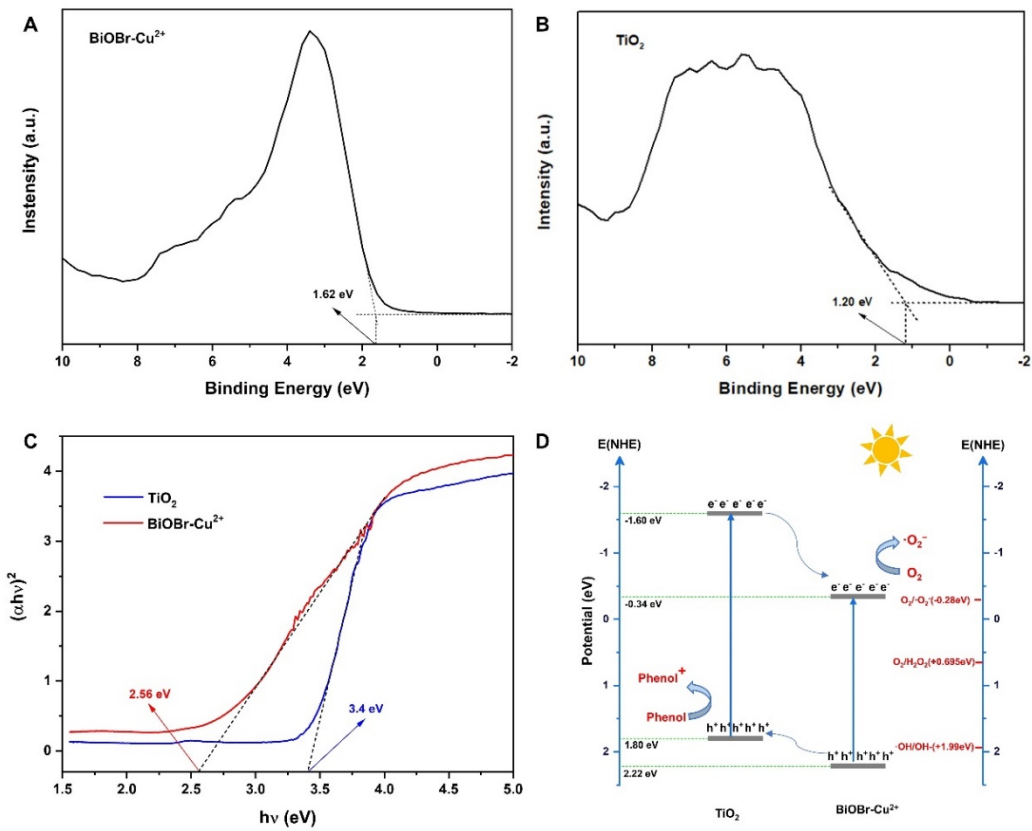


Figure S6. XPS valence-band spectra of BiOBr-Cu^{2+} (A) and TiO_2 (B); Tacu's plot (C) of BiOBr-Cu^{2+} , TiO_2 ; Possible photocatalytic reactions (D) of $\text{BiOBr-Cu}^{2+}/\text{TiO}_2$ heterojunctions

Table S1 The model parameters of pseudo-first order, pseudo-second order, and intraparticle diffusion kinetics.

Kinetic models	Parameters	BiOBr-Cu ²⁺ /TiO ₂
<i>pseudo-first-order</i>	$Q_{e,f}^a$ (mg g ⁻¹)	2.98
	k_1 (min ⁻¹)	0.0837
	R^2	0.993
<i>pseudo-second-order</i>	$Q_{e,s}^a$ (mg g ⁻¹)	3.58
	k_2 (g mg ⁻¹ min ⁻¹)	0.222
	v_0 (mg g ⁻¹ min ⁻¹)	0.352
Intraparticle diffusion	R^2	0.994
	k_i (mg L ⁻¹ min ^{1/2})	0.310
	C_i	0.886
	R^2	0.931

Table S2 Comparison of the phenol adsorption and photocatalytic degradation between BiOBr-Cu²⁺/TiO₂ and other adsorbents reported in the literatures.

Adsorbent	Adsorption		Photodegradation				Ref.
	Adsorption capacity, mg g ⁻¹	Equilibrium time, min	Initial concentration, mg L ⁻¹	Degradation degree, %	Treatment time, min	Degradation rate, min ⁻¹	
BiOBr-Cu ²⁺ /TiO ₂	2.91	40	10	85.0	180	9.6 × 10 ⁻³	This work
TiO ₂ /ZnAl	0.15	120	10	55.7	120	6.0 × 10 ⁻³	[R1]
γ-Al ₂ O ₃ TiO ₂	— ^a	60	40	-	360	2.5 × 10 ⁻³	[R2]
ZnAl LDH-SDS	x ^b	60	40	95.0	420	-	[R3]
01%Pd-0.5%Au/TiO ₂	-	120	94.11	69	120	5.5 × 10 ⁻³	[R4]

^a means it is not mentioned or calculated.

^b represents almost no adsorption

References

- [R1] J.C. Contreras-Ruiz, S. Martínez-Gallegos, J.L. García-Rivas, J. Illescas, J.C. González-Juárez, G. Macedo Miranda, E. Ordoñez Regil, Influence of the textural parameters of LDH-TiO₂ composites on phenol adsorption and photodegradation capacities, Int. J. Photoenergy 2019 (2019) 1–11.
- [R2] C. Martinez-Gómez, I. Rangel-Vazquez, R. Zarraga, G. Del Ángel, B. Ruíz-Camacho, F. Tzompantzi, E. Vidal-Robles, A. Perez-Larios, Photodegradation and mineralization of phenol using TiO₂ coated γ-Al₂O₃: effect of thermic treatment, Processes 10 (2022) 1186.
- [R3] G. Romero Ortiz, L. Lartundo-Rojas, J.E. Samaniego-Benítez, Y. Jiménez-Flores, H.A. Calderón, A. Mantilla, Photocatalytic behavior for the phenol degradation of ZnAl layered double hydroxide functionalized with SDS, J. Environ. Manage. 277 (2021) 111399.
- [R4] M.T. Yilleng, E.C. Gimba, G.I. Ndukw, I.M. Bugaje, D.W. Rooney, H.G. Manyar, Batch to continuous photocatalytic degradation of phenol using TiO₂ and Au-Pd nanoparticles supported on TiO₂, J. Environ. Chem. Eng. 6 (2018) 6382–6389.